A Study of Three-Dimensional Histogram Using the NOAA AVHRR Images

Jun-ichi Kudoh and Shoichi Noguchi

Abstract—**As part of the fundamental studies of the multiple image processing, we have been developing the NOAA AVHRR three-dimensional analysis system, in which we encountered the problem of drawing the three-dimensional histogram on the two-dimensional CRT. In this case there are two factors: One is the coordinate position given by the brightness level of the three image channels of NOAA AVHRR, the other is the frequency of the points within the images. In order to decide the semi-optimum value to display the processed three-dimensional histogram, we tried to relate between frequency and the total number of pixels. We found that standard deviation of them is reasonable. In the results of analysis using this method, the difference of major components of images are displayed in the three-dimensional histogram. And thus we were able to identify the features of the histogram corresponding to the physical entities like, sea, land, cloud, etc. by a process known as clustering.**

I. Introduction

RECEPTION and analysis of NOAA satellite [1] data has been studied by the faculty of science of Tohoku University since 1988. Parts of that data have been stored in the image data base at the computer center, available to the network named TAINS of Tohoku University. NOAA images are a significant theme in the study of image processing [2].

The images obtained from the Advanced Very High Resolution Radiometer (AVHRR) aboard the NOAA satellite are composed of multi-spectral images, which have four or five different wavelength bands, the analysis of which, in essence, require four- or five-dimensional simultaneous spatial analysis. But the presentation of the results is limited to the three dimensions of vision. There have been only a few studies [3] on three-dimensional analysis of remote sensing, due to unavailability of high performance computers, suitable softwares, and technical methods.

In the case of analysis of the multi-spectral images, we analyzed the NOAA AVHRR images by using a three-dimensional histogram. We found that semi-optimum clusters of the histogram were obtained by the standard deviation of the three-image frequency which was used in statistical method. We propose a new method to analyze the NOAA AVHRR images. And we also have shown that practical use of CH3 in the morning is possible by using our method.

Manuscript received October 18, 1990; revised January 24, 1991.

The authors are with the Research Center for Applied Information Science, Tohoku University, Japan.

IEEE Log Number 9101252.

II. Three-Dimensional Histogram

The three-dimensional histogram technique is a method of displaying the brightness (0–255) of the three images from the three different channels of NOAA to the three X, Y, and Z axes of a graph. This histogram expresses the information of the images at the same time, so that it is possible to extract property information or clustering of the subject explicitly.

The three images are image1, image2, and image3. The length and breadth of an image is described as x and y. The brightness of the pixel is I_1, I_2, and I_3, which corresponds to the three images of image1, image2, and image3. In this study three-dimensional spatial distribution means the brightness distribution of I_1, I_2, and I_3. As all the images from CH1 to CH4 have 512 × 512 pixel and 256 levels, the ranges of (x, y) and $[I_1, I_2, I_3]$ are as follows:

$$(0, 0) \le (x, y) \le (511, 511) \tag{1}$$

$$[0, 0, 0] \le [I_1, I_2, I_3] \le [255, 255, 255] \tag{2}$$

where, ( ) is coordinates of the length and breadth of an image, [ ] is the axis of coordinates of the brightness of image1, image2, and image3. In these three images the pixel number P, which is counted by scanning the images, and corresponds to α_1, α_2, and α_3 of the images, is described by (3).

$$P[I_1, I_2, I_3] = \sum_{x=0}^{511} \sum_{y=0}^{511} \delta\{\alpha_1, I_1(x, y)\} \cdot \delta\{\alpha_2, I_2(x, y)\} \cdot \delta\{\alpha_3, I_3(x, y)\} \tag{3}$$

$$[0, 0, 0] \le [\alpha_1, \alpha_2, \alpha_3] \le [255, 255, 255]. \tag{4}$$

The range of P is described by (5):

$$0 \le P \le 512 \times 512 \tag{5}$$

where, $\delta\{i, j\} \equiv \delta_{ij}$ is Kronecker's Delta.

The distribution of P corresponds to the components of images, which depend on the physical properties of three channels. Thus the distribution of P in the three bright-

0196-2892/91/0900-0736$01.00 © 1991 IEEE

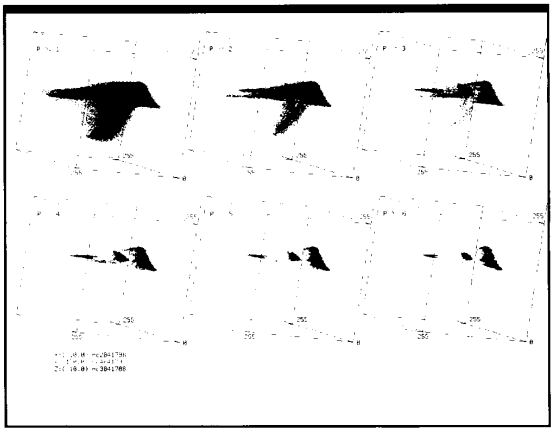

Fig. 1. Change of histograms with P functions.

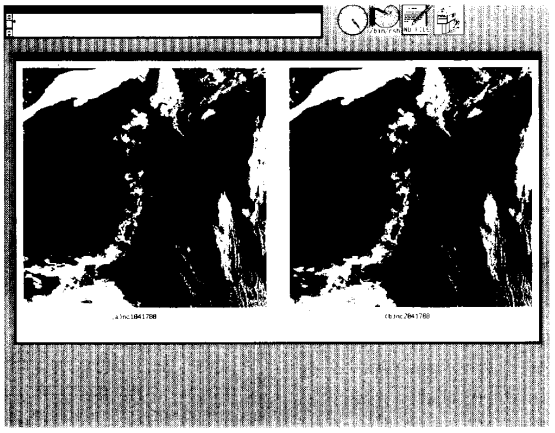

(a) (b)

Fig. 2. NOAA AVHRR images of the example sample: (a) CH1, (b) CH2.

ness spatial distributions is obtained by scanning all the areas of $\alpha_1 \sim \alpha_3$.

The problem in this case is that in order to draw the three-dimensional histogram on the two-dimensional CRT, two factors are considered; one is the coordinate position given by the brightness of the three images channels; the other is the frequency of similar points.

Fig. 1 shows the change of the histogram shapes by P of (3). The sample scene shown in Figs. 2 and 3 will be discussed later. In Fig. 1 the X, Y, and Z axes correspond to CH2, CH4, and CH3, respectively. This presentation is the rotation of the X-axis by $-10°$, the Y-axis is by 150°, and the Z-axis by $-10°$ at the origin, respectively. This histogram presents the clusters which correspond to characteristic information by AND operation of the three images. In the cases of $P \geq 1$, all the points of histogram are displayed, but the interface between each cluster is unclear (see Fig. 1). As the value of P increases, the points in that histogram decrease. In the case of $P \geq 6$, although it is possible to identify the clusters easily, the significant information has been lost.

Kudoh *et al.* [4] tried to display the three-dimensional histogram of the color-scale by using the multi-spectral images of an x-ray microanalyzer [5], whose images are obtained by a similar principle of remote sensing. But the method is too vague to use in this analysis.

In this paper we propose a method to decide the semi-optimum value of P in (1) for the three-dimensional histogram of NOAA AVHRR images.

III. NOAA AVHRR Images

The properties of multi-spectral images of NOAA AVHRR are as follows:
CH1(λ = 0.58–0.68 μm: visible); CH2(λ = 0.73–1.10 μm: near-infrared); CH3(λ = 3.55–3.93 μm: infrared); CH4(λ = 10.5–11.5 μm: infrared); CH5(λ = 11.5–12.5 μm: infrared). The target location is a region called TO-

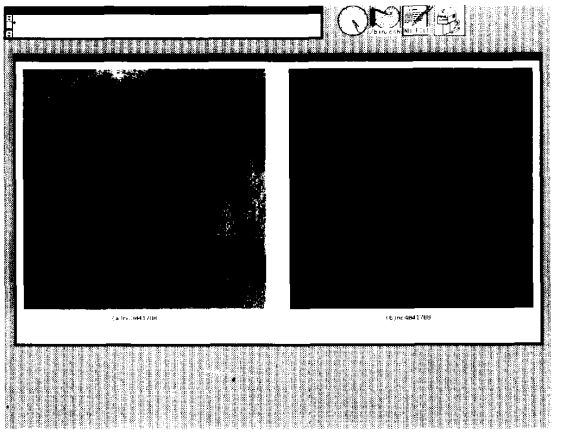

(a) (b)

Fig. 3. NOAA AVHRR images of the example sample: (a) CH3, (b) CH4.

HOKU, located north of TOKYO (JAPAN), and the original image area is 1024 × 1024 pixels (1 pixel is about 1.1 km) about the center of TOHOKU.

The data obtained from the target channel, CH1 to CH4, were converted into images by Mercator projection and CH4 was converted into the brightness-temperature of the images by the science faculty of Tohoku University. Although one pixel of the original data is 2 b, it is normalized to 1 b because of the requirement of the huge memory size of the computer. If one pixel of data is 2 b, it needs 1024^3 b. In the case of one pixel of 1 b, it needs 256^3 b memory. Taking into account the memory size and processing time required, all the pictures are thinned out to 512 × 512 pixels, because the computer display size is 1152 × 900 dots.

A. Picture Noise

Figs. 2 and 3 show the example scenes images corresponding to CH1 to CH4, respectively, which were obtained from NOAA-10 satellite. We cannot recognize the picture noise of CH1, CH2, and CH4. However, CH3 has a little periodic noise, but is not beyond the scope of analysis.

B. Combination of Three Channels

There are four sets of combinations of three channels from CH1 to CH4. As CH3 contains more noise than other channels, and because in the wavelength band of CH3 we have radio-infrared and infrared reflect, it is difficult to include CH3 in analysis [7].

The first combination considered is CH1, CH2, and CH4. In this case, CH3 is not included. CH1 and CH2 are suitable for land analysis, since the CH1 is in the chlorophyll absorption band and the CH2 is within the infrared reflectance band, which is very sensitive to the amount of vegetation and its condition.

The second combination is CH2, CH3, and CH4. In this case, CH3 is included. In the daytime, usage of CH3 is not easy because of both emitted thermal and reflected solar contributions to the upwelling radiance of sun [8]. We mention in section V-B that CH3 also shows the ability to classify the image components using this method in spite of its difficulty.

IV. Taking the Statistics

There are three quantities used as parameters beside P in order to display the three-dimensional histogram. Table I lists these parameters. The one is $A(P)$, which is the sum of all points in the image, for the value of P from P to inifinity. The second is $H(P)$, which is sum of all points in the three-dimensional histogram, for the value of P from P to infinity. The third is $\Delta H(P)$, which is the difference of $H(P$, i.e., $\Delta H(P) = H(P) - H(P + 1)$.

In this case, the image size is 512 × 512. But the subject area is different for different users. So this size is considered flexible. For this reason, $A(P)$ cannot be considered an appropriate parameter. From the statistical point of view, $\Delta H(P)$ is considered to be more appropriate because $\Delta H(P)$ is a function of P, not $H(P)$. Here, σ is the standard deviation of $\Delta H(P)$.

A. Data for Statistics

Fig. 4 shows the 12 scenes of CH2 which are analyzed in this report. Here, each image of Fig. 4 was thinned out to 256 × 256 pixels, in order to display the 12 pictures at the same time in this paper. They are of fine days in the Japan area. The pictures are chosen from the period of February to the end of October in 1989. The total data set used was 24, because of the combination of the three image channels mentioned previously.

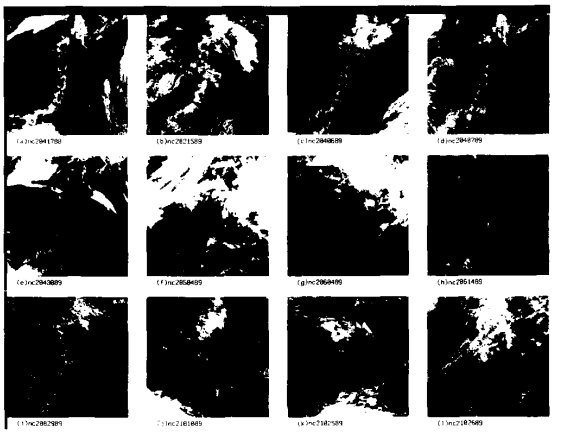

Fig. 4. All NOAA AVHRR images of CH2 used calculations.

TABLE I
RESULTS OF $A(P)$, $H(P)$, AND $\Delta H(P)$ OF THE EXAMPLE SAMPLE, AND STANDARD DEVIATION OF $\Delta H(P)$.

P	$A(P)$	$H(P)$	$\Delta H(P)$
≥ 1	262144	106631	70821
≥ 2	191323	35810	16704
≥ 3	157915	19106	6292
≥ 4	139039	12814	3095
≥ 5	126659	9719	1981
≥ 6	116754	7738	1333
≥ 7	108756	6405	930
≥ 8	102246	5475	745
≥ 9	96286	4730	567
≥ 10	91183	4163	433
≥ 11	86853	3730	362
≥ 12	82871	3368	290
≥ 13	79391	3078	249
≥ 14	76154	2829	229
≥ 15	72948	2600	207
≥ 16	69843	2393	197
≥ 17	66691	2196	180
≥ 18	63631	2016	182
≥ 19	60355	1843	144
≥ 20	57619	1690	128
≥ 21	55059	1562	—
			$\sigma = 2.388$

TABLE II
RESULTS OF STANDARD DEVIATION OF THE USED IMAGES DATA

No.	Data	CH1,2,4	CH2,3,4
1	'88.04.17	2.176	2.388
2	'89.02.15	3.083	1.944
3	'89.04.06	1.126	1.812
4	'89.04.07	2.674	2.746
5	'89.04.30	3.355	2.523
6	'89.05.04	3.197	1.567
7	'89.06.04	2.195	1.805
8	'89.06.14	3.567	3.005
9	'89.08.29	2.366	2.085
10	'89.10.10	2.670	1.994
11	'89.10.25	3.258	2.085
12	'89.10.26	2.608	1.903
	Av.(σ)	2.773	2.155
		2.464	

B. Calcuation of Results

Table I list the calculated results of the data of Figs. 2 and 3. It was found that the standard deviation is 2.388. Table II lists the standard deviations of all data. The average standard deviation is 2.464.

V. DISCUSSION

We found by the statistics that the semi-optimum value of P is between 2 and 3. With reference to Table I, if we chose the value of $P \geq 2$, the total number of pixels lost $\Delta H(P)$ is 70821, which is about 27% of the total pixels obtained, i.e., 262144 and used in the case of $P = 1$. For $P \geq 3$, the amount of unutilized pixel is (262144 − 157915) = 104229, which is about 40% of the total pixels obtained. Thus considering the lost image information, the value $P \geq 2$ is better than $P \geq 3$.

A. Distribution of Out of Range Information

Fig. 5 shows the distribution of out-of-range information for the case of $P = 1$ over the CH2 with red points.

In this case, measured data was from April 17, 1988, at seven o'clock in the morning, Japanese time. At this time, the snow was covering part of the mountains, with morning fog in the basin area and over part of the sea. Thus the major image components of CH2 are sea, land, snow, fog, and cloud. In Fig. 5 we found that the red points are distributed over all components, but are especially concentrated at the interface of the image components.

From Fig. 1 we can observe that the interface between clusters is seen more easily for $P \geq 2$ than for $P \geq 1$. In this example, we could use $P \geq 3$ in the analysis, but as

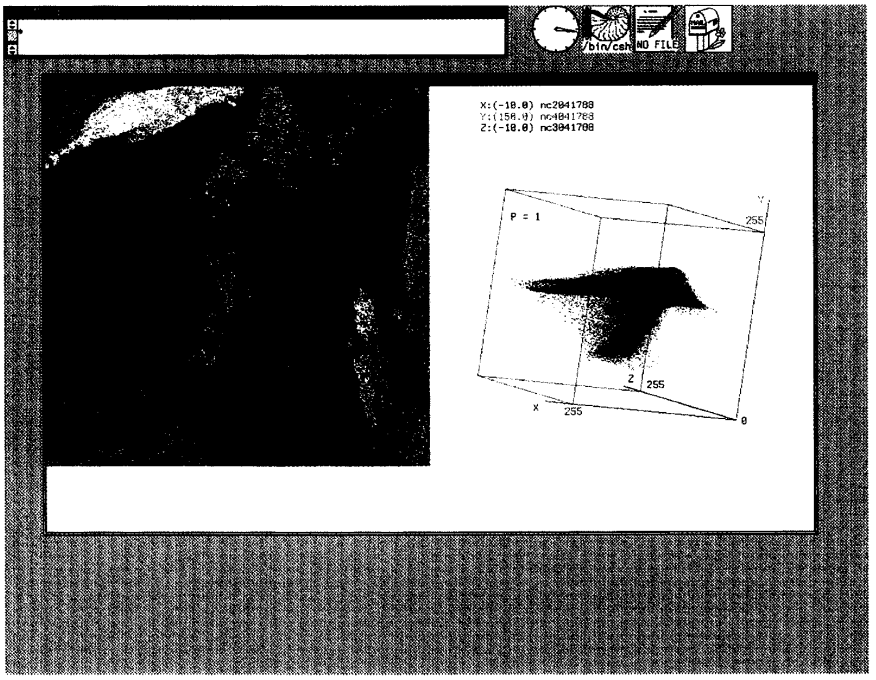

Fig. 5. Distribution of $P = 1$ overlaid CH2 image.

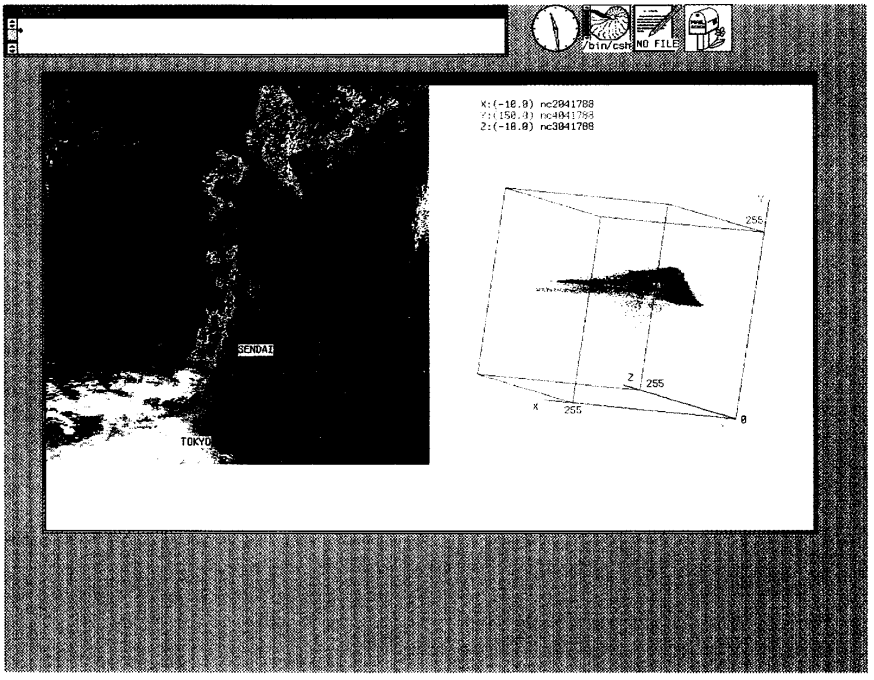

Fig. 6. Clustering results by using three-dimensional analysis.

previously mentioned, lost pixels in the case $P \geq 3$ correspond to about 40% of total pixels. So it seems that $P \geq 2$ is better than $P \geq 3$ for active utilization of more image information.

B. Applied to Clustering

Fig. 6 shows the results of clustering of Figs. 2 and 3, by using the method of three-dimensional histograms for $P \geq 2$. In Fig. 6 sea, land, snow, fog, cloud, and Kuroshio Front are painted over the CH2 by light blue, gray, red, green, yellow, and magenta, respectively. These colors correspond to a three-dimensional histogram. The aim of this clustering is to distinguish each image component, for example, the sea can be distinguished in more detail. In Fig. 6, the axes of the three-dimensional histogram X, Y, and Z correspond to CH2, CH4, and CH3, respectively. As the image of CH2 is in the visible range, it is difficult to distinguish the features of snow, fog, and cloud, because of the apparent whiteness of them. These features, however, can be distinguished by clustering in this histogram method. We would like to mention that in the construction of Fig. 6 we have used CH3, and that the effect of its noise is negligible which is important in determining different features.

In this example, the determination of areas of snow, fog, cloud, and Kuroshio Front was obtained by cross-reference to the data of local observed information [9].

C. Calculation Results

In this study, the three-dimensional histogram was made under the condition, $P \geq 2$ from (1). In the computer, (1) is called 256^3 times in the histogram-making routine program. But in reality for this example, it has been called only 4180 times, which took about 2 min to execute.

In Table I, the average of $\Delta H(P)$ is 5253, so it corresponds to P between 3 and 4. This value is greater than the results of the standard deviation ($P = 2$). If we use $P = 3$ or $P = 4$, the lost information data of image increases. From a viewpoint of active use of image data, the standard deviation method is a better than average one.

VI. Conclusion

We have determined the semi-optimum value P of three-dimensional histograms by analyzing three NOAA AVHRR images simultaneously, as the standard deviation. It is necessary for developing a more complete three-dimensional analysis system of NOAA. This system is intended to have a better human–machine interface.

Acknowledgment

A debt of gratitude is extended to Prof. H. Kawamura and Dr. H. Kaminaga (Tohoku University), who provided NOAA image data.

References

[1] J. C. Barnes and M. D. Smallwood, "TIROS-N/NOAA Series Direct Readout Services Users Guide," U.S. Department of Commerce of NOAA, 1982.

[2] H. Kaminaga, J. Kudoh, and S. Noguchi, "A support system for analyzing NOAA images," *Papers Annual Meet, The Inst. Electronics, Inf. & Comm. Eng. Japan*, D-535, pp. 7–287, 1990.

[3] C. E. Livingstone, K. P. Singh, and A. L. Gray, "Seasonal and regional variations of active/passive microwave signatures of sea ice," *IEEE Trans. Geosci. Remote Sensing*, vol. GE-25, no. 2, March, pp. 159–173, 1987.

[4] J. Kudoh, Y. Sasaki, and K. Yoshino, "Image analysis system of x-ray micro analyzer," *J. Inst. Image Electron. Eng. Japan*, vol. 18, no. 5, pp. 313–318, 1989.

[5] J. Kudoh, S. Noguchi, A. Tsuchiyama, and M. Kitamura, "Automatic classification method for multiple images," *Proc. 40th Annual Conventions ISP Japan*, 5E-2, pp. 374–375, 1990.

[6] L. Lauritson, G. J. Nelson, and F. W. Porto, "Data extraction and calibration of TIROS-N/NOAA radiometers," NOAA Tech. Memo. NESS1077, 1979.

[7] K. Akaeda and T. Takeda, "The utilization of NOAA 7 AVHRR Channel 3 data to infer the cloud structure," *TENKI*, vol. 30, no. 1, pp. 53–58, 1984.

[8] M. Takagi, "Receiving system for meteorological satellite (NOAA)," *Bull. Airborne and Satellite Phys. & Fish. Oceanogr.*, vol. 6, pp. 51–63, 1983.

[9] S. Obata, S. Matsuzawa, and H. Kawamura, "A nature of TOHOKU from the view of cosmos," *SENAC*, vol. 22, no. 3, 1989.

Jun-ichi Kudoh, photograph and biography appear on p. 709 of this issue.

Shoichi Noguchi, photograph and biography appear on p. 709 of this issue.